Journal of Information Hiding and Multimedia Signal Processing ©2017 ISSN 2073-4212
Ubiquitous International Volume **8**, Number **2**, March **2017**

Power Loss Analysis of AC Contactor at Steady Closed State with Electromagnetic-Thermal Coupling Method

Shuyi Lin and Xiaosheng Huang

Fujian Provincial Key Laboratory of Digital Equipment
Fujian University of Technology
No.3, Xueyuan Road, University Town, Minhou, Fuzhou, 350118, China
linshuyi1985@qq.com;huangxiaosheng2010@qq.com

Received May, 2016; revised December, 2016

Abstract. *AC contactor is a kind of widely applied low-voltage apparatus. Almost all of power losses occur during the closed state, so the power losses of AC contactor at the closed state are the key to realizing energy-saving. The coil of AC contactor can be energized by alternating or direct current. For the latter case, there are hysteresis and eddy-current losses caused by alternating magnetic field, which makes the electromagnetic-thermal analysis quite difficult and low accuracy. In this paper, FEM (Finite Element Method) is applied to analyse a kind of AC contactor, which is applied in air condition, with high accuracy. The power losses and temperature distribution of AC contactor at closed state with different kind of coil excitation are simulated through electromagnetic-thermal coupling method. The simulation data with high accuracy provides theoretical basis for energy and material saving of AC contactor.*
Keywords: AC contactor, FEM, Electromagnetic-thermal, Power losses, Closed state.

1. **Introduction.** AC contactor is a kind o f low-voltage apparatus which is applied to close and open circuit frequently,and it maintains the closed state for most of the time. Coil of AC contactor can be energized by alternating or direct current. For the latter case, there are hysteresis and eddy-current losses caused by alternating magnetic field, which make the electromagnetic-thermal analysis quite difficult and low accuracy. In theory, any conductor of the AC contactor will generates eddy-current loss.The conductive parts include the main coil, shading coil, magnetic core. Moreover, there is also hysteresis loss in the magnetic cores. All the losses will cause temperature rise, which will affect losses at the same time. Therefore, the electromagnetic-thermal analysis of AC contactor at closed state is quite important and difficult.

As a traditional method, the Newton Formula is usually applied for calculating the steady temperature rise of coil. However, many factors which affect the power losses are ignored, the accuracy of traditional method is very low. Heat circuit method is quite simple with smaller amount of computation, but the accuracy is low. With the development of computer and simulation technology, more and more scholars apply FEM to calculate thermal field of electromagnetic mechanism [1–11]. However, the temperature calculation of AC contactor is actually electromagnetic-thermal coupling field more than pure thermal field. Therefore, the accuracy of present AC contactor simulation can be improved. This paper proposes an electromagnetic-thermal coupling method to calculate the power losses and 3D temperature distribution of AC contactor at the steady closed state with both AC and DC coil excitation cases. The calculation accuracy of temperature rise is improved significantly, and the simulation results with high accuracy provide theoretical basis for energy and material saving of AC contactor.

2. **Electromagnetic-Thermal Coupling Mathematical Model of AC Contactor in the Steady Closed State.**

2.1. **Power Loss Calculation Model of AC Contactor in the Steady Closed State.** The electromagnetic mechanism and its corresponding model is shown in Fig.1. The prototype includes moving core, static core, shading coil, main coil, skeleton and so on.

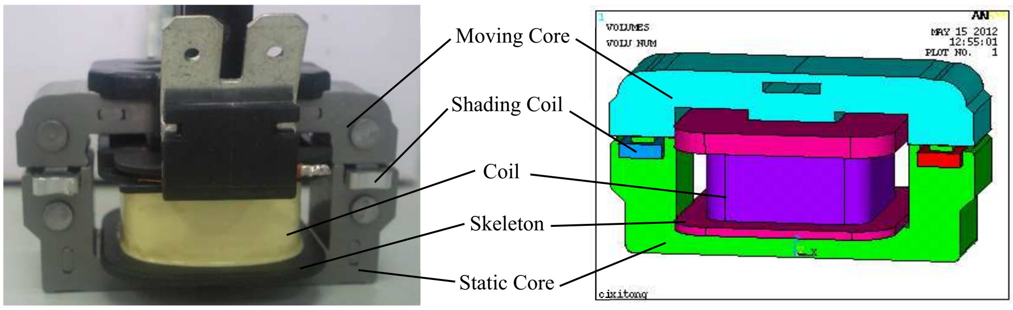

FIGURE 1. Mechanical model of AC contactor (left) and its 3D model (right)

When the coil of AC contactor is excited by AC current, there will be magnetic hysteresis loss and eddy-current caused by alternate magnetic field.The hysteresis loss in each finite element of magnetic core is calculated by:

$$P_{he} = fV_e \int_{BHl} dH_e dB_e \tag{1}$$

where P_{he} is magnetic hysteresis loss of finite element, f is frequency, V_e is volume of the finite element, BHl is the B-H hysteresis loop, H_e is magnetic field intensity of the finite element, B_e is magnetic flux density of the finite element [1]. The hysteresis loops of magnetic material is provided by the manufacturer.

The whole area of hysteresis loop is less than $4H_{em}B_{em}/3$, where H_{em} is the maximum magnetic field intensity, B_{em} is the maximum magnetic flux density. Therefore, for each element, the hysteresis loss is less than $4fV_eH_{em}B_{em}/3$. The total hysteresis loss is the sum of each element, and it is less than $4f\sum_{i=1}^{n}(V_eH_{em}B_{em})/3$, where n is the total number of element. From the built FEM model of AC contactor, the total magnetic hysteresis loss $P_h < 0.0372W$, and it takes the proportion of total power losses is less than 1.43%. Therefore, the hysteresis loss can be ignore in this model. Therefore, the main heat source includes coil loss, eddy-current loss of moving and static core and the shading coil loss.

The model can be divided into eddy current area and no eddy current area according to the conductive of material. Therefore, moving core, static core, shading coil are belong to eddy current area, and the other parts are belong to no eddy current area [12–14]. For the eddy current area, method based on the vector magnetic potential and scalar electric potential can be applied, and the control formulas are:

$$\nabla \times \frac{1}{\mu} \times \boldsymbol{A} - \nabla \frac{1}{\mu} \nabla \cdot \boldsymbol{A} + \gamma \frac{\partial \boldsymbol{A}}{\partial t} + \sigma \nabla V = 0 \tag{2}$$

$$\nabla \cdot (-\gamma \frac{\partial \boldsymbol{A}}{\partial t} - \gamma \nabla V) = 0 \tag{3}$$

where γ means conductivity, μ is permeability, V is scalar potential, $\boldsymbol{A}$ is magnetic vector potential, t means time. The control formula of no eddy current area is:

$$\nabla \times \frac{1}{\mu} \times \boldsymbol{A} - \nabla \frac{1}{\mu} \nabla \cdot \boldsymbol{A} = \boldsymbol{J}_s \tag{4}$$

where $\boldsymbol{J}_s$ is current density of coil. According to the Maxwell equation and the definition of magnetic vector potential, there are the formulas as following:

$$\nabla \times H = \boldsymbol{J} \tag{5}$$

$$\boldsymbol{H} = \frac{1}{\mu} \boldsymbol{B} \tag{6}$$

$$\boldsymbol{B} = \nabla \times \boldsymbol{A} \tag{7}$$

where $\boldsymbol{H}$ is magnetic field intensity,$\boldsymbol{B}$ is magnetic flux density, $\boldsymbol{J}$ is current density.

2.2. **Thermal Field Calculation Model of AC Contactor at the Steady Closed State.** The heat energy, which is caused by power losses of AC contactor, usually dissipates through conduction, convection and radiation. According to the national standard, the magnitude of allowed temperature rise of electric appliance is limited to 10^2, and the radiant power is negligible. Therefore, it just considers conduction and convection in this paper. Heat dissipation can be handled through surface coefficient of heat transfer in the FEM model, and the conduction equation is:

$$\rho C_p \frac{\partial \theta}{\partial t} - \nabla \cdot (\lambda \nabla \theta) - S = 0 \tag{8}$$

where ρ means density, C_p is specific heat capacity, θ is temperature, λ is heat conductivity, S is heat generation rate [1]. The boundary conditions of heat dissipation is:

$$-\lambda \frac{\partial \theta}{\partial \boldsymbol{n}} = \alpha(\theta_0 - \theta_f) \tag{9}$$

where α is surface coefficient of heat transfer,θ_0 is temperature of heating element, θ_f is the environment temperature.

2.3. **Electromagnetic-Thermal Coupling Calculation of AC Contactor at the Steady Closed State.** The heat energy, which makes the temperature rise of each parts, is caused by eddy current loss and coil loss. According the equations 5-7, the current density $\boldsymbol{J}$ is calculated by:

$$\boldsymbol{J} = \nabla \times \frac{1}{\mu} \nabla \times \boldsymbol{A} \tag{10}$$

Then, the heat generation rate S can be calculated by:

$$S = \frac{1}{\sigma} |\boldsymbol{J}|^2 \tag{11}$$

As illustrated in Fig.2, first, setting the environment temperature, material property of each part, exciting voltage, simulation time t_{end}, time step Δt and so on. Heat generation rate S of coil, cores and shading coil with the variation of time can be got by 11. Making S as the heat excitation of each part in the thermal field model, which is solved by 8 and 9. Then, the temperature distribution at $t + \Delta t$ can be got. If $t + \Delta t < t_{end}$, the material property of each part will be updated according the new temperature distribution. Making

$t = t + \Delta t$, and repeating the process until $t = t_{end}$. Finally, save the result and turn to the post process.

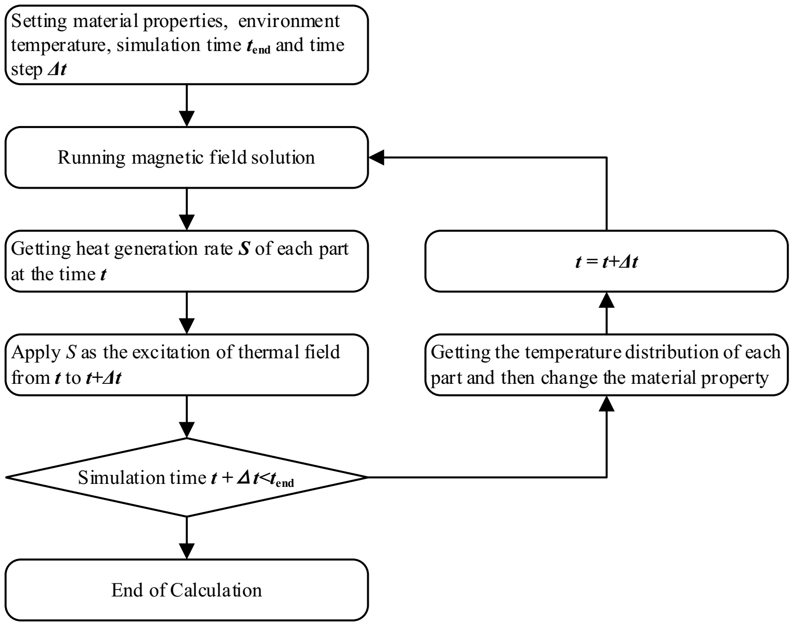

Figure 2. Calculation flow chart of electromagnetic-thermal coupling

3. **Experimental Verification of FEM Model.** Temperature rise with different voltage was tested. The rated voltage is 220V at 50Hz, and the environment temperature is 28°C. The comparisons of simulation and measurement is illustrated in Table 1, where U-voltage, P-power, L-inductance, ΔT-temperature rise, and U_e-the rated voltage. The maximum relative error of power and inductance are 6.5% and 2.48% respectively. And the maximum relative error of average temperature of coil is 5.41%. The results of simulation and measurement match well.

Table 1. Comparisons of simulation and measurement

U/U_e	P(W)			L(H)			ΔT(K)		
	FEM	Exp.	Error	FEM	Exp.	Error	FEM	Exp.	Error
0.8	1.55	1.47	5.44%	22.83	23.41	2.48%	31.4	30.1	4.32%
0.9	2.13	2.00	6.50%	21.51	20.05	2.45%	40.9	38.8	5.41%
1	2.76	2.61	5.75%	20.80	20.77	0.14%	52.0	50.7	2.56%
1.1	3.61	3.48	3.74%	19.32	19.43	0.57%	69.1	68.7	0.58%

3.1. **Electromagnetic-Thermal Simulation of AC contactor with AC-energized coil.** The 3D heat generation rate result of each part is illustrated in Fig.3, with $T_e = 65.6$°C, and $U = 1.1U_e$ at 50Hz.

Heat generation rate equal to the ratio of power losses and volume. Fig.3 shows that the heat generation rate of cores is mainly focus on the middle column of cores. The heat generation rate of coil is quite uniform. Coil is the main heat source and it takes 72.63% of the total power losses. Core loss takes 24.47% of that. Meanwhile, the loss of static core is more than moving core.

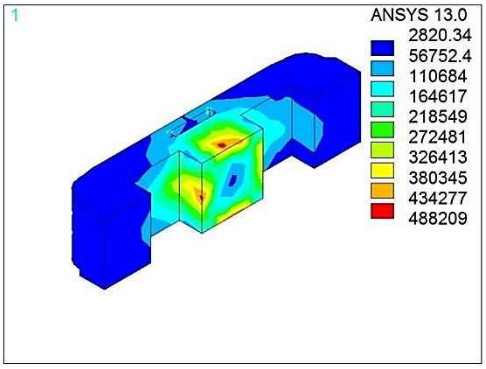

(a) Moveing core

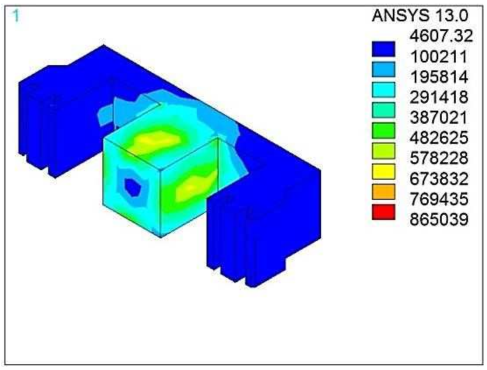

(b) Static core

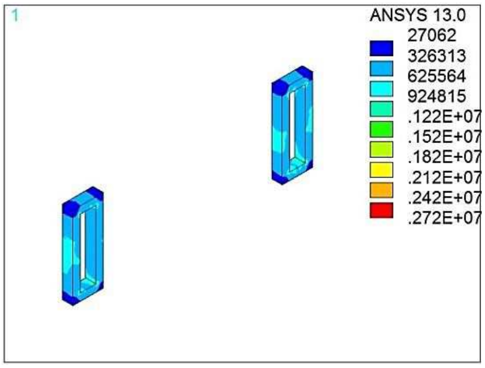

(c) Shading coil

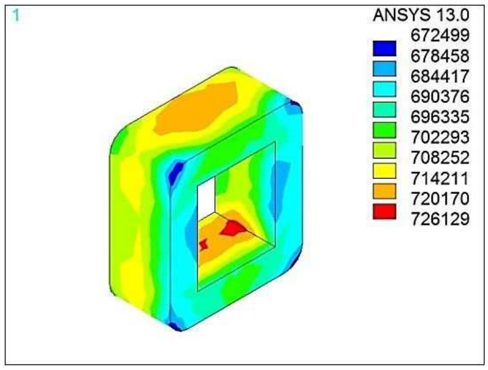

(d) Coil

FIGURE 3. 3D heat generation rate of each part

3.2. **Electromagnetic-Thermal Simulation of AC contactor with DC-energized coil.** Through the built 3D model of AC contactor, the lowest holding voltage is about 15V. Therefore, setting the holding voltage as 22V for considering the appropriate margin. Setting simulation environment temperature as 65.6°Cand the result of 3D heat generation rate of AC contactor is showed in Fig.4.

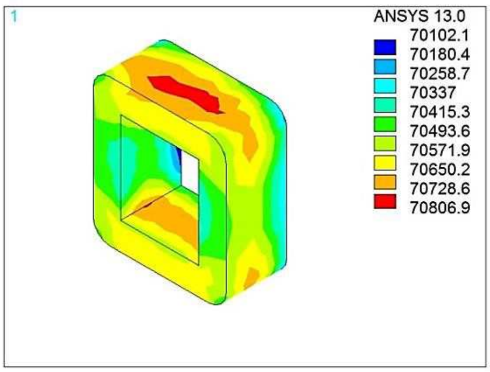

FIGURE 4. 3D heat generation rate of coil at 22V DC holding voltage

The power losses of coil are the only heat source at closed state when the main coil is energized by DC voltage. The heat generation rate of DC energized coil is just one-sixth of the AC energized coil. The power losses of coil are just 0.2743W, and its temperature rise is decreased sharply. Meanwhile, the total power losses of AC contactor are also decreased significantly.

4. **Power Loss of AC Contactor at the Closed State.**

4.1. **Power Loss Analysis of AC Contactor at Closed State with AC-energized Coil.**

Defining the initial parameters as: coil turn $N = 5620$, wire diameter $d = 0.08mm$, rated voltage $Ue = 220V$. For the AC-energize case, the power losses of coil and cores take the most of total power losses. Therefore, we focus on the analysis of power losses with the variation of coil parameters and thickness of cores. The highest allowed operation temperature is 155°C according to the grade F of coil heat-resisting. When the environment temperature is 65.6°C and the input voltage is $1.1U_e$, the long term average temperature rise must be less than 89.4K. For appropriate margin, the long term average temperature rise should be less than 80K. Setting the environment temperature to 65.6°C, the input voltage $U = 1.1U_e$. And then running the simulation with the variation of parameters. The simulation results and the data analysis are as follow.

Table 2 shows the power losses and temperature rise with the variation of turns N form 4800 to 6000. In the table, P_d is power losses of moving core, P_j is power losses of static core, P_{sc} is power losses of shading coil, P_w is power losses of coil, I means current, and S means apparent power.

Table 2. Power loss and temperature rise with the variation of coil turns

$U = 1.1U_e$						$U = U_e$		
N	P_d/W	P_j/W	P_w/W	P_{sc}/W	ΔT_{avg}/K	I/mA	S/VA	EEG
6000	0.23	0.63	2.11	0.096	57.75	27.22	5.99	2
5800	0.24	0.64	2.50	0.10	66.17	28.94	6.37	2
5620	0.25	0.68	2.76	0.11	72.08	31.31	6.89	2
5400	0.27	0.72	3.30	0.12	81.89	34.06	7.49	2
5200	0.27	0.74	4.00	0.12	95.84	37.11	8.16	2
5000	0.28	0.76	5.02	0.13	115.02	40.29	8.86	3
4800	0.30	0.77	5.78	0.13	130.51	44.51	9.79	3

The result shows that: the percentage of coil power losses increases with the decrease of coil turns. When $N < 5400$, the temperature rise will reach the highest allowed temperature rise. With the increase of N, the apparent power increases clearly. All the EEG (Energy Efficiency Grades) are 2 within the allowed temperature rise range. When $N < 5200$, the EEG will reach to 3. Therefore, the effect of energy and material saving by changing the coil turns is not apparent.

Table 3 shows the power losses and temperature rise with the variation of wire diameter d form 0.06mm to 0.08mm. The result shows that: the percentage of coil power losses increases with the decrease of wire diameter. When $d <$ 0.071mm, the temperature rise will reach to the highest allowed temperature rise. With the decrease of d, the apparent power decreases. The EEG keeps 2 with the variation of wire diameter within the allowed temperature rise range. Therefore, the energy and material saving won't change much with the variation of wire diameter.

Table 4 shows the power losses and temperature rise with the variation of core thickness H_t from 10.0mm to 12.5mm.

The result shows that: with the decrease of H_t, power losses of cores and shading coil decrease obviously and the percentage of coil power losses increases. When $Ht <$ 11.5mm, the temperature rise will reach to the highest allowed temperature rise. With the decrease of H_t, the apparent power increase clearly. All the EEG are 2 within the range of allowed temperature rise. When $Ht <$ 10.0mm, the EEG will reach 3. According to the analysis

TABLE 3. Power loss and temperature rise with the variation of wire diameter

	$U = 1.1U_e$					$U = U_e$		
d/mm	P_d/W	P_j/W	P_w/W	P_{sc}/W	ΔT_{avg}/K	I/mA	S/VA	EEG
0.085	0.26	0.69	2.60	0.11	67.21	31.86	7.01	2
0.080	0.25	0.68	2.76	0.11	72.08	31.31	6.89	2
0.075	0.25	0.65	2.97	0.10	75.61	30.90	6.80	2
0.071	0.24	0.63	3.24	0.10	82.43	30.26	6.66	2
0.065	0.22	0.60	3.53	0.093	90.28	29.86	6.57	2
0.063	0.22	0.60	3.59	0.088	92.89	29.55	6.50	2
0.060	0.21	0.55	3.82	0.084	93.94	29.15	6.41	2

TABLE 4. Power loss and temperature rise with the variation of wire diameter

	$U = 1.1U_e$					$U = U_e$		
H_t/mm	P_d/W	P_j/W	P_w/W	P_{sc}/W	ΔT_{avg}/K	I/mA	S/VA	EEG
12.5	0.29	0.71	2.17	0.10	59.42	28.33	6.23	2
12.0	0.27	0.68	2.56	0.11	68.05	30.32	6.67	2
11.5	0.25	0.62	3.10	0.11	79.31	31.81	7.00	2
11.0	0.24	0.60	3.75	0.084	92.81	33.12	7.29	2
10.0	0.19	0.50	5.15	0.073	122.01	38.65	8.50	3

above, the EEG keeps 2 for the AC-energized case within the allowed temperature rise range. The eddy current losses take one half of the total power losses, and the apparent power is high. The EEG won't reach 1 ($S < 0.5$VA) by changing coil diameter, turns, and core thickness. If the main coil is energized by DC voltage , there will be no eddy current losses and the contactor can keep closed with a very low DC voltage. There will be only coil loss, energy-saving of contactor can be realized.

4.2. **Power Loss Analysis of AC Contactor at Closed State with DC-energized Coil.** Table 5 shows the simulation results with the variation of holding DC voltage at 65.6°C environment temperature.

TABLE 5. Simulation results of AC contactor at different DC voltage

U/V	$\Delta T_{avg-dtx}$/K	$\Delta T_{avg-jtx}$/K	ΔT_{avg-gj}/K	ΔT_{avg-xq}/K	I/mA	$Power$/W
15.4	2.71	2.83	4.10	4.73	8.86	0.14
17.6	3.38	3.53	5.16	5.97	10.08	0.18
19.8	4.09	4.28	6.32	7.33	11.29	0.22
22	4.91	5.15	7.74	9.01	12.50	0.27
24.2	5.60	5.87	8.89	10.35	13.67	0.33
26.4	6.43	6.75	10.31	12.03	14.83	0.39

In the table, $\Delta T_{avg-dtx}$ is average temperature of moving core, $\Delta T_{avg-jtx}$ is average temperature of static core, ΔT_{avg-gj} is average temperature of skeleton, ΔT_{avg-xq} is average temperature of coil, I means coil current. The result shows that the maximum coil average temperature rise is 12.03K, which is far below the limit of allowed temperature rise. The power is less than 0.5W, and the EEG keeps 1. It realizes the energy saving of contactor.

Table 6 shows the power losses and temperature rise with the two coil energized methods.

Table 6. Power loss and temperature rise with the variation of wire diameter

AC energizing			DC energizing			Ratio of S
U_{AC}/V	ΔT_{avg-xq}/K	S/VA	U_{DC}/V	ΔT_{avg-xq}/K	S/VA	
154	26.43	3.20	15.4	4.73	0.14	4.38%
176	34.33	4.22	17.6	5.97	0.18	4.27%
198	43.51	5.42	19.8	7.33	0.22	4.06%
220	55.50	6.89	22.0	9.01	0.27	3.92%
242	72.08	8.81	24.2	10.35	0.33	3.75%
264	103.54	11.53	26.4	12.03	0.39	3.38%

In the table,U_{AC} is effective value of AC holding voltageU_{DC} is DC holding voltage, Ratio of S means the ratio of apparent power between DC and AC energizing methods. The result shows that all the apparent power at closed state with DC-energized coil is less than 5% that of AC-energized coil. And the ratio will be decreased with the increase of voltage. Without changing the original structure of contactor, the temperature rise of coil with DC-energized coil is far less than that of AC-energized coil. The temperature rise of coil with low DC holding voltage is less than 20K, which is far less than 80K.

The wire diameter and coil turns, which will affect the temperature rise directly, are the keys of energy and material saving. Setting the environment temperature as 65.6°C, wire diameter as 0.08mm, and the DC holding voltage as 24.4V.Table 7 shows the simulation results with the variation of coil turns from 5500 to 500.

Table 7. Power loss and temperature rise with the variation of wire diameter

N	5500	4500	3500	2500	1500	1000	750	500
P_{xq}/W	0.338	0.431	0.577	0.846	1.337	1.944	2.502	3.541
ΔT_{avg}/K	10.61	13.55	18.44	24.50	44.02	63.89	81.85	113.89
I/mA	14.0	17.8	23.91	35.15	55.29	80.34	103.44	146.41
R/ω	1725.2	1353.1	1008.6	685.0	437.51	301.1	233.86	165.19
S/VA	0.339	0.431	0.579	0.851	1.338	2.081	2.503	3.543
EEG	1	1	2	2	2	2	2	2

In the table, P_{xq} means power dissipation of coil. The result shows that when $N < 750$, the average temperature rise is close to the critical temperature rise. Therefore, when wire diameter is 0.08mm, coil turns must be more than 750, and the thermal property can be satisfied. When coil turns is less than 3500, the apparent power will exceed 0.5W, and the EEG will reduce to 2. Thus there are two critical turns $N_{critial}$. One is the critical turn according to the thermal property and another is according to the EEG from 1 to 2. Table 8, 9 shows the two critical turns in different wire diameters.

Table 8 shows that the apparent power larger than 2W considering the critical turns according to thermal property. Although the EEG keeps 2, the copper of coil and the apparent power are decreased significantly. Fig.5 shows the two critical turns with the variation of coil diameter.

Curve 1 shows the critical coil turns between EEG 1 and EGG 2. Curve 2 shows the critical turns according to thermal property. There are three area A, B, C shown in Fig.5

Table 8. Power loss and temperature rise with the variation of wire diameter

U	d	$N_{critial}$	P_{xq}/W	ΔT_{avg}/K	I/mA	R/ω	S/VA	EEG
24.2	0.07	600	2.44	81.76	100.77	240.08	2.47	2
24.2	0.08	750	2.50	81.85	103.44	233.86	2.50	2
24.2	0.09	900	2.59	81.49	106.87	226.36	2.59	2
24.2	0.10	1050	2.67	80.88	110.38	219.13	2.67	2
24.2	0.12	1280	2.96	80.73	122.87	196.22	2.97	2
24.2	0.15	1580	3.34	80.64	138.16	174.91	3.34	2

Table 9. Power loss and temperature rise with the variation of wire diameter

U	d	$N_{critial}$	P_{xq}/W	ΔT_{avg}/K	I/mA	R/ω	S/VA	EEG
22	0.06	2050	0.50	10.71	22.7	967.2	0.50	1
22	0.07	2850	0.50	15.38	22.7	965.2	0.50	1
22	0.08	3400	0.50	15.35	22.7	964.1	0.50	1
22	0.09	3950	0.50	15.06	22.7	968.2	0.50	1
22	0.10	4450	0.50	14.17	22.7	967.3	0.50	1

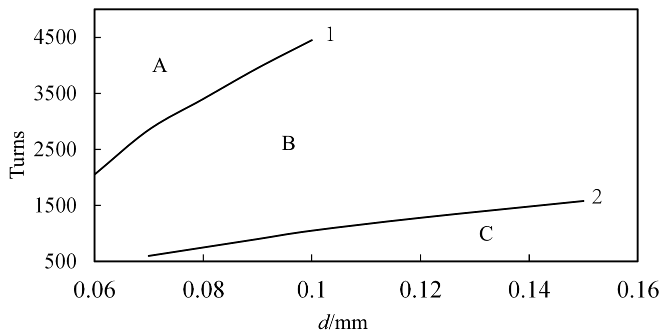

Figure 5. The two critical turns with the variation of coil diameter

for any state with DC-energized coil. When coil parameters stay in area A, the EEG keeps 1 with better thermal property. When coil parameters stay in area B, the EEG of contactor will decline to 2 with appropriate thermal property. However, the copper of coil is decreased significantly. If coil parameters stay in area C, the thermal property is unsatisfied.

5. **Conclusion.** This paper proposes an electromagnetic-thermal coupling method, which considers eddy current loss, resistivity of coil, coefficient of heat conduction and emission. It is suitable for the power losses analysis of AC contactor at closed state. The method is verified by simulation and experiment. The simulation results with high accuracy provides theoretical basis for energy and material saving of AC contactor. Meanwhile, two critical turns curves are proposed for coil parameters optimization and realizing the requested EEG at DC-energized case. The power losses, apparent power, EEG, temperature distribution with the variations of wire diameter, coil turns and core thickness are analyzed. The results show that in the range of allowed temperature rise, the EEG keeps 2 with AC-energized coil. For the AC-energized case, there are eddy current losses,which take one half of the total power losses, and EEG can't reach 1 by only changing coil diameter, turns, and core thickness. On the other hand, for the DC-energized case, there is no eddy

current losses, and the contactor can keep closed by a low DC-energized voltage. The temperature rise of DC-energized contactor decreases significantly. The EEG can reach 1 due to the very low apparent power, which takes 5% that of AC-energized case. The DC-energized method helps energy and material saving of AC contactor.

Acknowledgment. This work is supported by the National Natural Science Foundation of China (51607039), the Scientific Research Starting Foundation of Fujian University of Technology, China (GY-Z14074,GY-Z160005) and the Scientific Research & Development Foundation of Fujian University of Technology, China (GY-Z15102, GY-Z160122).

REFERENCES

[1] H.-C. Huang and A. S. Usmani, *Finite element analysis for heat transfer : theory and software*. London ; New York: Springer-Verlag, 1994.

[2] X. Guan, N. Shu, B. Kang, Q. Yan, Z. Li, H. Li, and X. Wu, Multi-physics calculation and contact degradation mechanism evolution of gib connector under daily cyclic loading, *IEEE Transactions on Magnetics*, vol. 52, no. 3, pp. 1–4, 2016.

[3] G. Liu, H. Liu, and B. Zheng, Thermal simulation of small capacity ac contactor based on ansys, in *Electrical Contacts (ICEC 2012), 26th International Conference on*, pp. 479–483, 2012.

[4] Z. Guan, L. I. Jiao, Y. Cui, L. I. Juan, and B. Huang, Thermal simulation of a contactor with feedback controlled magnet system, *Ieice Transactions on Electronics*, vol. 93, no. 9, pp. 1424–1430, 2010.

[5] C. P. Niu, D. G. Chen, Y. Y. Liu, and R. C. Dai, Thermal simulation of ac contactor considering the heat generated by main circuit and electromagnet system, *Proceedings of the Csee*, vol. 27, no. 15, pp. 53–58, 2007.

[6] C. Niu, D. Chen, X. Li, W. Tong, and Y. Geng, Thermal analysis of ac contactor using thermal network finite difference analysis method(session 7 -modeling-), *Ieice Technical Report Emd*, vol. 107, pp. 149–154, 2007.

[7] F. Serteller and M. A. Atalay, Thermal analysis of ferromagnet actuator by finite element method, *Physica B: Condensed Matter*, vol. 372, no. 1C2, pp. 366–368, 2006.

[8] K. Preis, O. Biro, G. Buchgraber, and I. Ticar, Thermal-electromagnetic coupling in the finite-element simulation of power transformers, *IEEE Transactions on Magnetics*, vol. 42, no. 4, pp. 999–1002, 2006.

[9] C. P. Niu, D. G. Chen, and L. P. Zhu, Simulation of thermal field for ac electromagnetic contactor, *Low Voltage Apparatus*, 2005.

[10] C.-J. Park, S.-S. Kim, B.-H. Chun, S.-H. Kim, and D.-S. Doh, The heat transfer characteristics in air-lift contactor with activated carbon for the separation of air pollutants, *Korean Journal of Chemical Engineering*, vol. 19, no. 5, pp. 833–837, 2002.

[11] Y. Kawase, T. Ichihashi, and S. Ito, Heat analysis of thermal overload relays using 3-d finite element method, *IEEE Transactions on Magnetics*, vol. 35, no. 3, pp. 1658–1661, 1999.

[12] O. Biro and K. Preis, On the use of the magnetic vector potential in the finite-element analysis of three-dimensional eddy currents, *IEEE Transactions on Magnetics*, vol. 25, no. 4, pp. 3145–3159, 1989.

[13] W. Renhart, H. Stogner, and K. Preis, Calculation of 3d eddy current problems by finite element method using either an electric or a magnetic vector potential, *Magnetics IEEE Transactions on*, vol. 24, no. 1, pp. 122–125, 1988.

[14] D. Albertz and G. Henneberger, Calculation of 3d eddy current fields using both electric and magnetic vector potential in conducting regions, *IEEE Transactions on Magnetics*, vol. 34, no. 5, pp. 2644–2647, 1998.